



## **Can toxicokinetic and toxicodynamic modeling be used to understand and predict synergistic interactions between chemicals?**

Cedergreen, Nina; Dalhoff, Kristoffer; Li, Dan; Gottardi, Michele; Kretschmann, Andreas Christopher

*Published in:*  
Environmental Science & Technology (Washington)

*DOI:*  
[10.1021/acs.est.7b02723](https://doi.org/10.1021/acs.est.7b02723)

*Publication date:*  
2017

*Document version*  
Publisher's PDF, also known as Version of record

*Citation for published version (APA):*  
Cedergreen, N., Dalhoff, K., Li, D., Gottardi, M., & Kretschmann, A. C. (2017). Can toxicokinetic and toxicodynamic modeling be used to understand and predict synergistic interactions between chemicals? *Environmental Science & Technology (Washington)*, 51(24), 14379-14389.  
<https://doi.org/10.1021/acs.est.7b02723>

# Can Toxicokinetic and Toxicodynamic Modeling Be Used to Understand and Predict Synergistic Interactions between Chemicals?

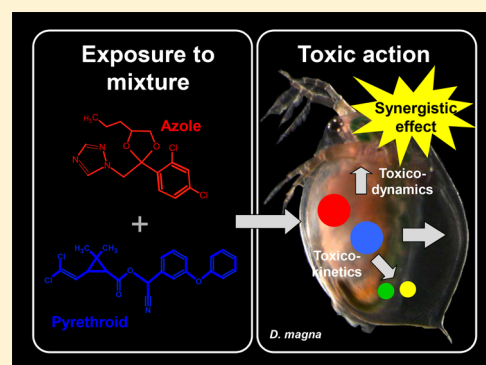
Nina Cedergreen,<sup>\*,†,‡</sup> Kristoffer Dalhoff,<sup>†,‡</sup> Dan Li,<sup>†,§</sup> Michele Gottardi,<sup>†,‡</sup> and Andreas C. Kretschmann<sup>†,‡</sup>

<sup>†</sup>Department of Plant and Environmental Science, University of Copenhagen, Thorvaldsensvej 40, 1871 Frederiksberg C, Denmark

<sup>‡</sup>Toxicology Lab, Department of Pharmacy and Analytical Biosciences, University of Copenhagen, Universitetsparken 2, 2100 Copenhagen Ø, Denmark

**S** Supporting Information

**ABSTRACT:** Some chemicals are known to enhance the effect of other chemicals beyond what can be predicted with standard mixture models, such as concentration addition and independent action. These chemicals are called synergists. Up until now, no models exist that can predict the joint effect of mixtures including synergists. The aim of the present study is to develop a mechanistic toxicokinetic (TK) and toxicodynamic (TD) model for the synergistic mixture of the azole fungicide, propiconazole (the synergist), and the insecticide,  $\alpha$ -cypermethrin, on the mortality of the crustacean *Daphnia magna*. The study tests the hypothesis that the mechanism of synergy is the azole decreasing the biotransformation rate of  $\alpha$ -cypermethrin and validates the predictive ability of the model on another azole with a different potency: prochloraz. The study showed that the synergistic potential of azoles could be explained by their effect on the biotransformation rate but that this effect could only partly be explained by the effect of the two azoles on cytochrome P450 activity, measured on *D. magna* in vivo. TKTD models of interacting mixtures seem to be a promising tool to test mechanisms of interactions between chemicals. Their predictive ability is, however, still uncertain.



## INTRODUCTION

Some chemicals are known to enhance the effect of other chemicals beyond what can be predicted with standard mixture models, such as concentration addition and independent action. These chemicals are called synergists. Up until now no models exist that can predict the joint effect of mixtures including synergists. Azole fungicides have been shown to act as synergists in a range of studies, enhancing the toxicity of pyrethroid insecticides up to 10–50-fold in a range of organisms.<sup>1–4</sup> Also other pesticide or biocide combinations have shown to induce repeatable synergy in a range of organisms.<sup>5</sup> Synergy and antagonism between chemicals can occur through a range of mechanisms: first, one chemical can affect the availability of another chemical outside an organism through either precipitation or change in speciation, as it has been demonstrated for metals in mixtures.<sup>6–8</sup> Second, one chemical can affect the uptake rate of another chemical, for example, by enhancing penetration<sup>9</sup> or by facilitating availability by enhancing ventilation rates in aquatic organisms.<sup>10</sup> Third, one chemical can affect the transport of another chemical to its target, as it is often observed in plants,<sup>11</sup> or a chemical can affect the biological action of other chemicals by either inhibiting or promoting their transformation through interactions with biotransformation enzymes such as cytochrome P450 monooxygenases and esterases.<sup>12,13</sup> Finally, chemicals can

compete for a common target site or affect the excretion of one another.

In a review of synergistic interactions, 95% of all documented pesticide synergies were caused by either azole fungicides or carbamate and organophosphate insecticides, known to inhibit cytochrome P450 monooxygenases and/or esterases.<sup>5</sup> Hence, for pesticide mixtures, it seems as if interactions involving biotransformation of other pesticides are the main mechanism behind the observed synergies. Despite this hypothesis often being cited, very little direct evidence exists proving that inhibition or activation of biotransformation of other chemicals is the single most important mechanism of synergy of azole fungicides, carbamate, and organophosphate insecticides.<sup>3,10,14–16</sup> For azole/pyrethroid interactions, for example, Chalvet-Monfrey et al. found that the synergy of prochloraz on deltamethrin in bees could not be explained by effects on biotransformation alone<sup>17</sup> but that effects on uptake rates were also likely to take place.<sup>16</sup>

Synergists acting on biotransformation pathways could potentially be screened by using in vitro or in vivo assays for the effect of chemicals on different metabolic enzymes.<sup>12,18,19</sup>

**Received:** May 26, 2017

**Revised:** September 6, 2017

**Accepted:** September 13, 2017

**Published:** September 13, 2017

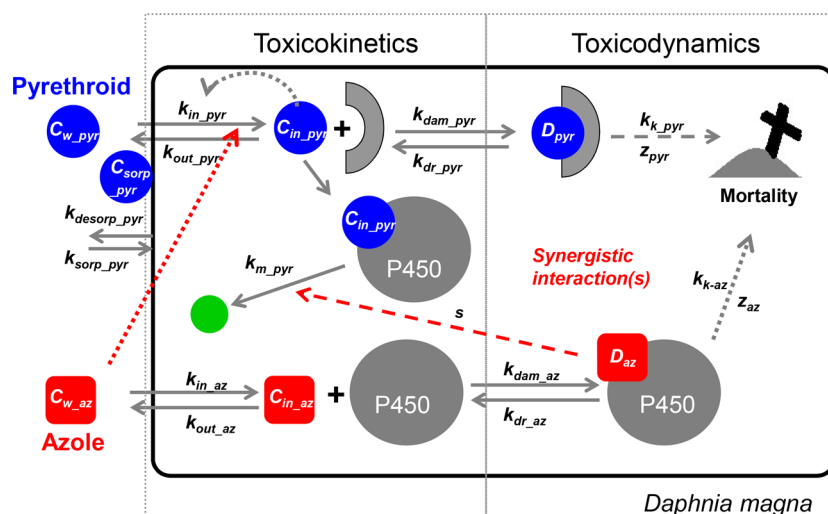


**Figure 1.** Conceptual model of the toxicokinetic (left side) and toxicodynamic (right side) processes of a pyrethroid insecticide and an azole fungicide and their interactions in *D. magna*, symbolized by the large square. Inside the daphnid, there are two targets for the pesticides: the sodium channel (gray half-circle), which is the target site of the pyrethroid, and P450 enzymes (gray circle), the main target site for the azoles. The pyrethroids act as substrates for the P450 enzymes when they are biotransformed (green circle). The state variables, describing how the amounts of pesticide in the different locations change over time, are given in blue circles for the pyrethroids and by red squares for the azoles, and are all described by differential equations given in the text. The rate constants, describing TK processes, are given next to the solid arrows denoting the specific processes (values are given in Table 1), while parameters relating damage to mortality, assuming GUTS-SD (eq 8 and 9), are given next to the gray dashed arrows. The synergistic interaction is proposed to occur when azoles bind to P450 enzymes, making them unavailable for pyrethroid biotransformation, thereby decreasing the rate by which the P450 enzymes can biotransform the pyrethroid (red dashed arrow). The alternative hypothesis for synergy, where azoles affect pyrethroid uptake rates, is denoted by a red dotted arrow. Mechanisms that are neglected in the first versions of the model but which might be of importance, such as direct effects of the azoles on daphnia mortality or effects on uptake rates due to the  $\alpha$ -cypermethrin damage done to daphnia mobility, are denoted by dotted gray arrows.

But even if a chemical is known to inhibit certain enzymes, the size of the potential synergistic interactions and its development over time cannot be quantified with any existing model approach.<sup>20</sup> A possible tool to test mechanisms of synergy and ultimately to predict the size of synergy over time are toxicokinetic (TK) and toxicodynamic (TD) models.<sup>21</sup> TK models predict uptake and elimination of chemicals over time and TD models predict the development of effects over time as a function of the modeled or measured internal chemical concentrations.<sup>21,22</sup> Mixture toxicity calculations using TKTD models have been proposed but only for noninteracting chemicals with similar molecular target sites.<sup>23</sup> TKTD models for interactive chemicals could be a tool to test hypotheses on the mechanism of interaction. If they are successful, they may also be used to predict the size of synergistic interactions under different exposure scenarios.

The aim of the present study is therefore three-fold: first, we wish to build and parametrize a full TKTD model for the synergistic interactions between the azole fungicide propiconazole (the synergist) and the pyrethroid insecticide  $\alpha$ -cypermethrin on the mortality of the crustacean *Daphnia magna* (Figure 1), when propiconazole is present at one constant concentration. Second, we wish to test the different hypotheses concerning the mechanism of synergy (effects on uptake versus the effect on biotransformation rate), and third, we will validate the model assumptions in terms of synergistic interactions with a synergist with a similar mode of action but different potency, the azole fungicide prochloraz. To confirm the hypothesis that the azoles induce synergy through interference with biotransformation, the model is parametrized to a data set with variable propiconazole or prochloraz concentrations, and the modeled effect on the biotransforma-

tion rate is compared with cytochrome P450 activity inhibition measured in vivo.

## METHODS

**Theory.** The conceptual model is shown in Figure 1. It is initially assumed that the uptake of the pyrethroid will follow a first-order kinetic uptake and elimination model, including a biotransformation rate constant,  $k_{m\_pyr}$ , describing the rate by which the pyrethroid is biotransformed in the organism.

$$\frac{dC_{in\_pyr}(t)}{dt} = k_{in\_pyr} \times C_{w\_pyr}(t) - k_{out\_pyr} \times C_{in\_pyr}(t) - k_{m\_pyr} \times C_{in\_pyr}(t) \quad (1)$$

In this equation, the change in internal pyrethroid concentrations,  $C_{in\_pyr}$ , in the daphnids over time is described as a function of the uptake rate,  $k_{in\_pyr}$ , the excretion rate,  $k_{out\_pyr}$ , the biotransformation rate,  $k_{m\_pyr}$  and the external pyrethroid concentration in the water,  $C_{w\_pyr}$ . Phase I biotransformation is, in the case of pyrethroids, believed mainly to be governed by P450 monooxygenases,<sup>24</sup> though esterases may also play a substantial role.<sup>24–26</sup> As pyrethroids are very hydrophobic ( $\log K_{ow} = 6.94$  at pH 7 for  $\alpha$ -cypermethrin), sorption to the daphnid exoskeleton could also be a process of quantitative significance. It is given in Figure 1 as  $C_{sorp\_pyr}$ , and the change over time of  $C_{sorp\_pyr}$  is proposed to be described with first-order kinetics using a sorption specific uptake and elimination rate constant,  $k_{sorp\_pyr}$  and  $k_{desorp\_pyr}$ , respectively:

$$\frac{dC_{sorp\_pyr}(t)}{dt} = k_{sorp\_pyr} \times C_{w\_pyr}(t) - k_{desorp\_pyr} \times C_{sorp\_pyr}(t) \quad (2)$$

Table 1. Toxicokinetic and Toxicodynamic Model Parameters and Their Definitions<sup>a</sup>

parameter	definition	unit	value
state variables			
$C_{in\_pyr}$	pyrethroid concentration inside the daphnia (eq 1)	pmol g <sup>-1</sup> FW	
$C_{sorp\_pyr}$	pyrethroid concentration sorbed to the daphnia (eq 2)	pmol g <sup>-1</sup> FW	
$D_{pyr}^*$	scaled damage by the pyrethroid given in the unit of $C_{in\_pyr}$ (eq 7)	pmol g <sup>-1</sup> FW	
$H_{pyr}$	cumulative hazard induced by the pyrethroid (eq 8)		
$S_{pyr}$	survival probability (eq 9)		
$C_{in\_az}$	azole concentration inside the daphnia (eq 3)	nmol g <sup>-1</sup> FW	
$D_{az}^*$	scaled damage by the azole given in the unit of $C_{in\_az}$ (as eq 7, but using $C_{in\_az}$ and $k_{dr\_az}$ )	nmol g <sup>-1</sup> FW	
variables			
$C_{w\_pyr}$	pyrethroid concentration in the water	nmol L <sup>-1</sup>	Figure 2B
$C_{in+sorp\_pyr}$	sum of $C_{in\_pyr}$ and $C_{sorp\_pyr}$	pmol g <sup>-1</sup> FW	Figure 2A
$C_{w\_az}$	azole concentration in the water	μmol L <sup>-1</sup>	
$s$	factor by which $k_{m\_pyr}$ is decreased in the presence of the azoles ( $0 < s < 1$ ) (eq 5)	–	PP <sup>b</sup> : 0.113 ± 0.058; PC <sup>b</sup> : < 0.001
constants			
$k_{in\_pyr}$	uptake rate constant of pyrethroid into daphnia tissue	h <sup>-1</sup>	46.5 ± 7.08
$k_{out\_pyr}$	elimination rate constant of pyrethroid out of daphnia tissue	h <sup>-1</sup>	<0.00001
$k_{m\_pyr}$	biotransformation rate constant of pyrethroid in daphnia	h <sup>-1</sup>	0.141 ± 0.038
$k_{sorp\_pyr}$	sorption rate constant of pyrethroid to daphnia surface	h <sup>-1</sup>	492 ± 133
$k_{desorp\_pyr}$	desorption rate constant of pyrethroid to daphnia surface	h <sup>-1</sup>	1.40 ± 0.47
$k_{dr\_pyr}$	damage repair rate constant for pyrethroid	h <sup>-1</sup>	Table S9
$k_{k\_pyr}$	killing rate constant for pyrethroid	g FW pmol <sup>-1</sup> h <sup>-1</sup>	Table S9
$h_b$	background hazard rate constant	h <sup>-1</sup>	0
$z_{pyr}$	threshold for effect of pyrethroid	h <sup>-1</sup>	Table S9
$k_{in\_az}$	uptake rate constant of azole into daphnia tissue	h <sup>-1</sup>	PP: 3.58; PC: 7.88
$k_{out\_az}$	elimination rate constant of azole out of daphnia tissue	h <sup>-1</sup>	PP: 0.233 ± 0.007; PC: 0.215 ± 0.018
$k_{dr\_az}$	damage repair rate constant for azole (× 10 <sup>-2</sup> )	h <sup>-1</sup>	PP: 1.08; PC: 2.23
$k_{k\_az}$	killing rate constant for azole (× 10 <sup>-4</sup> )	h <sup>-1</sup>	PP: 2.30; PC: 5.61
$z_{az}$	threshold for effect of azole	h <sup>-1</sup>	PP: 43.5; PC: 23.2
$b$	slope parameter for determining $s$ (eq 5)		PP: 3.36 ± 0.64; PC: 1.31 ± 0.07
$e$	azole concentration when $s$ is 0.5 (eq 5)	μM	PP: 0.060 ± 0.009; PC: 0.131 ± 0.003

<sup>a</sup>The state variables are defined by differential equations given in the text, and the variables either with equations or by nominal inputs as a function of time. All input data are given in Table S1–S8. The constants are given as the parameter estimates ± SE for TK parameters. Constants specific for propiconazole are marked with PP and for prochloraz with PC. The azole-specific TK parameters are taken from Dalhoff et al.,<sup>20</sup> while the TD parameters are re-fitted to raw data (Tables S4 and S5) to obtain the AIC values given in the text. <sup>b</sup>For the experiments with only one azole concentration, variable  $s$  could not be determined by a function but only with an azole concentration specific parameter.

The toxicokinetics of the azoles are described with a simplification of eq 1, only including an uptake and elimination rate constant,  $k_{in\_az}$  and  $k_{out\_az}$ .<sup>20</sup> The elimination rate constant in this equation therefore describes the sum of all biotransformation processes and efflux of the parent azole compound:

$$\frac{dC_{in\_az}(t)}{dt} = k_{in\_az} \times C_{w\_az}(t) - k_{out\_az} \times C_{in\_az}(t) \quad (3)$$

To test the hypothesis that the synergy is caused by the effect of the azole on the biotransformation rate, it was initially assumed that both pyrethroid uptake,  $k_{in\_pyr}$  and excretion,  $k_{out\_pyr}$ , were independent of the presence of the azole and that the only effect of the azole was on  $k_{m\_pyr}$ . As azoles bind to the catalytic site of the P450 enzymes, thereby prohibiting binding of the pyrethroid for biotransformation, we assume competitive inhibition of P450 enzymes by the azoles.<sup>27</sup> This means that the presence of azoles will decrease the amount of active P450 enzymes with a fraction depending on the internal azole concentration. This fraction is given by the parameter  $s$ . The parameter  $s$  can be defined by the ratio of the biotransformation

rate constant  $k_{m\_pyr}$  with and without coexposure to the azole under steady-state conditions.

$$s = \frac{k_{m\_pyr}(\text{coexposure})}{k_{m\_pyr}(\text{no coexposure})} \quad (4)$$

For a variable internal concentration of azoles, we expect  $s$  to vary according to the internal concentration of the azole,  $c_{in\_az}$ , following a sigmoidal function. We here describe the relationship with a log–logistic two-parameter model, where  $IC_{50}$  is the internal azole concentration inhibiting the biotransformation rate of the pyrethroid by 50% and  $b$  is the slope parameter of the curve:

$$s = \frac{1}{1 + (c_{in\_az}/IC_{50})^b} \quad (5)$$

We choose to use internal azole concentrations rather than scaled damage (eq 7) to describe  $s$ , as it can be measured experimentally. We recognize that the presence of the pyrethroid may also affect the activity of P450 monooxygenases. However, as the pyrethroid acts as a substrate for the P450 enzymes rather than as an inhibitor,<sup>28</sup> and in addition is



expected to occur at much lower internal concentrations compared to the azoles, we assume the quick catalytic biotransformation action will not significantly affect the total pool of P450 catalytic sites available. Hence, we chose not to include the pyrethroid's effect on P450 activity in the presented model.

The toxicodynamic part of the model describes the relation between internal pyrethroid concentrations and observed mortality. All azole concentrations included in the studies of synergy are chosen not to affect daphnid mortality ( $<EC_{10}^2$ ). Hence, mortality was assumed to depend on internal pyrethroid concentrations alone. Toxicodynamic parameters for the azoles are, however, inserted in Figure 1, and given in Table 1, as they have been determined in a previous publication<sup>20</sup> and will be used in the combined TKTD-model (Figure 1). Internal pyrethroid concentrations were related to mortality by including a damage stage, assuming that the pyrethroid insecticide induces some undefined damage with a rate,  $k_{\text{dam\_pyr}}$ , proportional to the internal pyrethroid concentration, and that the damage can be repaired by a rate,  $k_{\text{dr\_pyr}}$ , proportional to the size of the damage.

$$\frac{dD_{\text{pyr}}(t)}{dt} = k_{\text{dam\_pyr}} \times C_{\text{in\_pyr}}(t) - k_{\text{dr\_pyr}} \times D_{\text{pyr}}(t) \quad (6)$$

This is analogous to how internal chemical concentrations depend on external concentrations over time. In this case, however, we cannot measure damage directly. Pyrethroids inhibit the sodium channels of the nerves,<sup>28</sup> which will lead to a range of biochemical disruptions in the organism, which ultimately leads to immobilization and death. Because damage can rarely be measured directly, Jager et al. introduced the concept of scaled damage,  $D^*$ , which is proportional to the actual (but undefined) damage level, and has the unit of an internal concentration.<sup>21</sup> This is done by dividing eq 6 with the ratio of damage accrual and damage repair,  $k_{\text{dam\_pyr}}/k_{\text{dr\_pyr}}$ , thereby getting,

$$\frac{dD_{\text{pyr}}^*(t)}{dt} = k_{\text{dr\_pyr}} \times [C_{\text{in\_pyr}}(t) - D_{\text{pyr}}^*(t)] \quad (7)$$

The parameter  $k_{\text{dr\_pyr}}$  can be determined from the time course of survival of the test organisms. How damage relates to survival can be determined in two ways, representing extreme cases: one is assuming stochastic death above a certain damage threshold (the GUTS-SD model), the other is assuming that the organisms in the trial die, when they have exceeded an individual threshold for damage (the GUTS-IT model). For derivation, discussion, and testing of the two assumptions, we refer to Jager et al. and Ashauer et al.<sup>21,29–31</sup> Here we present the equations used to link scaled damage to survival under the assumption of stochastic death. For the individual threshold implementation and test, see SI B. For GUTS-SD, hazard to the organism,  $H_{\text{pyr}}$ , takes place when the damage increases above a certain threshold defined by  $z_{\text{pyr}}$ . Above  $z_{\text{pyr}}$ , hazard increases proportionally with the damage with a rate defined by the killing rate  $k_{\text{k\_pyr}}$ :

$$\frac{dH_{\text{pyr}}(t)}{dt} = k_{\text{k\_pyr}} \times \max[0, D_{\text{pyr}}^*(t) - z_{\text{pyr}}] \quad (8)$$

The survival probability as a function of time  $S_{\text{pyr}}(t)$  is calculated from the hazard, adding the background hazard ( $h_b$ ), derived from observations of control mortality:

$$S_{\text{pyr}}(t) = e^{-[H_{\text{pyr}}(t) + h_b(t)]} \quad (9)$$

With daphnids, it can be difficult to distinguish between immobility and death. In this study, we therefore define mortality as “immobility leading inevitably to death”. Hence, daphnids that have been categorized as immobile at one time point, but are then mobile at a subsequent time point, are included in the model as alive.

To build and parametrize the full TKTD model for the synergistic interactions between the pyrethroid  $\alpha$ -cypermethrin and an azole fungicide, several assumptions are made: first, the external  $\alpha$ -cypermethrin concentrations during the pulse exposure behave as described in Kretschmann et al.<sup>1</sup> by decreasing to 80% of nominal concentrations 0.5 h after spiking the compound to the medium and to 50% of nominal concentrations by the end of the pulse. This has been confirmed in independent, yet unpublished, experiments. Concerning toxicokinetics, we assume that  $\alpha$ -cypermethrin uptake follows first-order kinetics, as described for other organic chemicals,<sup>32</sup> that uptake rates are independent of external concentrations, also when the  $\alpha$ -cypermethrin pulse immobilizes the daphnids, and that P450 activity of daphnids is proportional to body weight before the onset of reproduction. The latter means that  $k_{\text{m\_pyr}}$  is constant within the time frame of the studies. For toxicodynamics, the main assumption is that all damage leading to daphnid mortality is caused by internal pyrethroid concentrations.

**Model Implementation.** The TKTD model was developed using the software OpenModel 2.4.2 (<http://openmodel.info/>) and the concepts described above and by Jager et al.<sup>21</sup> First, parameter values within realistic ranges giving model fits that visually described the data well were chosen as initial parameter values. Subsequently, parameters were optimized using the Marquardt method several times, choosing different starting values to ensure that a global minimum was reached during optimization. All model parameters were estimated by minimizing sums of squares, assuming normally distributed data, as OpenModel, in its present form, does not allow maximizing likelihood optimization routines. While normally distributed data are a valid assumption for the TK-data, it is not valid for the survival data. The parameter estimates will be similar using the different optimization procedures, but the error of the estimated parameters will not. Standard errors of the parameters are therefore only given for the TK-model. Different model fits were compared with Akaike's Information Criterion (AIC). For the TK-models, AIC was based on the Gaussian log-likelihood given by OpenModel, while for the TD-models, a multinomial log-likelihood was calculated according to Jager et al.<sup>21</sup> AIC was calculated as  $2k - 2\ln(L)$ , where  $k$  is the number of estimated parameters and  $\ln(L)$  is the calculated log-likelihood of the model. Test of significance between model fits were done by calculating the relative likelihood of model  $i$ . This was done by comparing the model with the lowest AIC ( $AIC_{\text{min}}$ ) to the AIC of model  $i$  by calculating  $\exp[(AIC_{\text{min}} - AIC_i)/2]$ . The calculated value can be interpreted as being proportional to the probability that the  $i$ th model minimizes the (estimated) information loss. If the value is  $<0.05$  then the two models are considered to be significantly different from each other.<sup>35</sup>

**Data.** The parametrization of the TK part of the model for the pyrethroid was based on measured internal concentrations of  $\alpha$ -cypermethrin with and without coexposure to propiconazole published in Kretschmann et al.,<sup>33</sup> while the TD part for

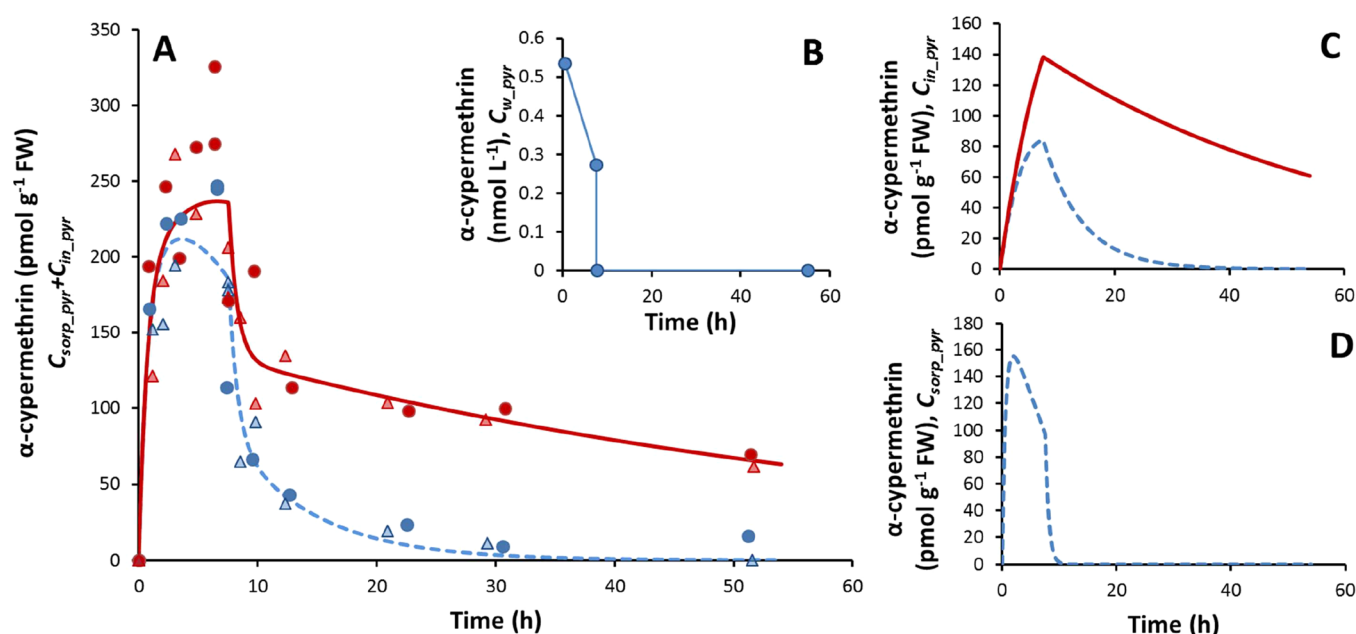


**Figure 2.** (A) shows the measured  $\alpha$ -cypermethrin concentrations in *D. magna* ( $C_{in\_pyr} + C_{sorp\_pyr}$ ) exposed to a 7.5 h pulse of  $\alpha$ -cypermethrin in the presence (red symbols and solid line) or absence (blue symbols and dashed line) of  $1.4 \mu\text{M}$  propiconazole. The circles and triangles represent data from two independent experiments. Data are described by eqs 1 and 2 and parameters are given in Table 1. The three  $\alpha$ -cypermethrin state variables are given in (B, C, and D): (B)  $\alpha$ -cypermethrin concentration in the water ( $C_{w\_pyr}$ ), given as measured data at time 0.5 and 7.5 h and the proposed zero concentration after removal to clean water, (C)  $\alpha$ -cypermethrin concentration inside the daphnid ( $C_{in\_pyr}$ ), and (D)  $\alpha$ -cypermethrin sorbed to the daphnid ( $C_{sorp\_pyr}$ ).

synergy between  $\alpha$ -cypermethrin and propiconazole and prochloraz was based on data published in Kretschmann et al.<sup>1</sup> The TKTD parameters and in vivo P450 inhibition data for both propiconazole and prochloraz were taken from Dalhoff et al.,<sup>20</sup> and the parametrization data for the synergy of low azole exposures were taken from Bjergager et al.<sup>34</sup> A short summary of the experiments and all raw data used to parametrize and validate the model are given in Tables S1–S8.

## RESULTS AND DISCUSSION

**Building the Toxicokinetic Model.** The model was built and parametrized on a data set with propiconazole as the synergist at one concentration known to yield maximal synergy and at a time point where equilibrium between the external medium and the daphnid was obtained.<sup>1,20</sup> Hence, in this version, the parameter  $s$  was a constant. As the measurements of internal  $\alpha$ -cypermethrin concentrations in the two independent experiments did not visually differ from each other (presented with different symbols in Figure 2 and in Table S1), both data sets were described with the same model. The measured internal  $\alpha$ -cypermethrin concentrations in the daphnids in the presence and absence of propiconazole were first described with a first-order uptake and elimination model, including a biotransformation rate constant,  $k_{m\_pyr}$  (eq 1). The model did not, however, describe the data well (AIC = 564, Figure S1). Due to high hydrophobicity of  $\alpha$ -cypermethrin, a sorption component was added (eq 2) and the sum of the two components  $C_{in\_pyr}$  and  $C_{sorp\_pyr}$  were fitted to the measured data. Rapid sorption and desorption processes were considered likely, as sorption and desorption experiments with  $\alpha$ -cypermethrin to a range of mineral and organic surfaces were shown to be very rapid, with halftimes in the range of 5–20 min.<sup>36</sup> This two-compartment model described data significantly better than the one compartment model (AIC = 503,

relative likelihood test,  $p < 0.001$ ), though it did not fully catch the high  $\alpha$ -cypermethrin concentrations measured during the pulse (Figure 2A). Letting the internal concentrations come from the sorbed fraction rather than from the water did not change this pattern and significantly decreased the goodness-of-fit (AIC = 520, relative likelihood test,  $p < 0.001$ ). One reason for not catching the high internal concentration during the pulse could be that we assume  $k_{m\_pyr}$  to be constant during the experiment. Other studies have shown induction of P450 activity of daphnids measured in vivo during both azole and  $\alpha$ -cypermethrin exposure within 18 h and up to several days.<sup>20,30</sup> If P450 induction takes place during the pulse exposure, then the best fit  $k_{m\_pyr}$ , which will basically be determined by data from the recovery phase, will overestimate the biotransformation rate during the exposure phase. Despite the model not catching the entire peak concentration in the daphnids, the decrease in internal concentrations over time was well-described. Hence, we used the parameters from this model, given in Table 1, in the following toxicodynamic models.

The hypothesis that azoles can enhance the uptake of a compound<sup>16</sup> (Figure 1, red-dotted arrow) was tested by including a specific uptake rate constant for the propiconazole treated daphnids. This extra parameter did not improve the fit (AIC = 510, relative likelihood test,  $p = 0.60$ ). Hence, it was concluded that the effect of propiconazole on internal concentrations was primarily through its effect on biotransformation rates of  $\alpha$ -cypermethrin.

**Building the Toxicodynamic Model.** The TD-models used the internal concentrations described by the TK model and were parametrized on the data set of immobility of daphnids over time exposed to pulses of a range of  $\alpha$ -cypermethrin, propiconazole, and prochloraz concentrations alone described in Kretschmann et al.<sup>1</sup> and in Dalhoff et al.<sup>20</sup> (Tables S2, S4, and S5). As the GUTS-SD model described

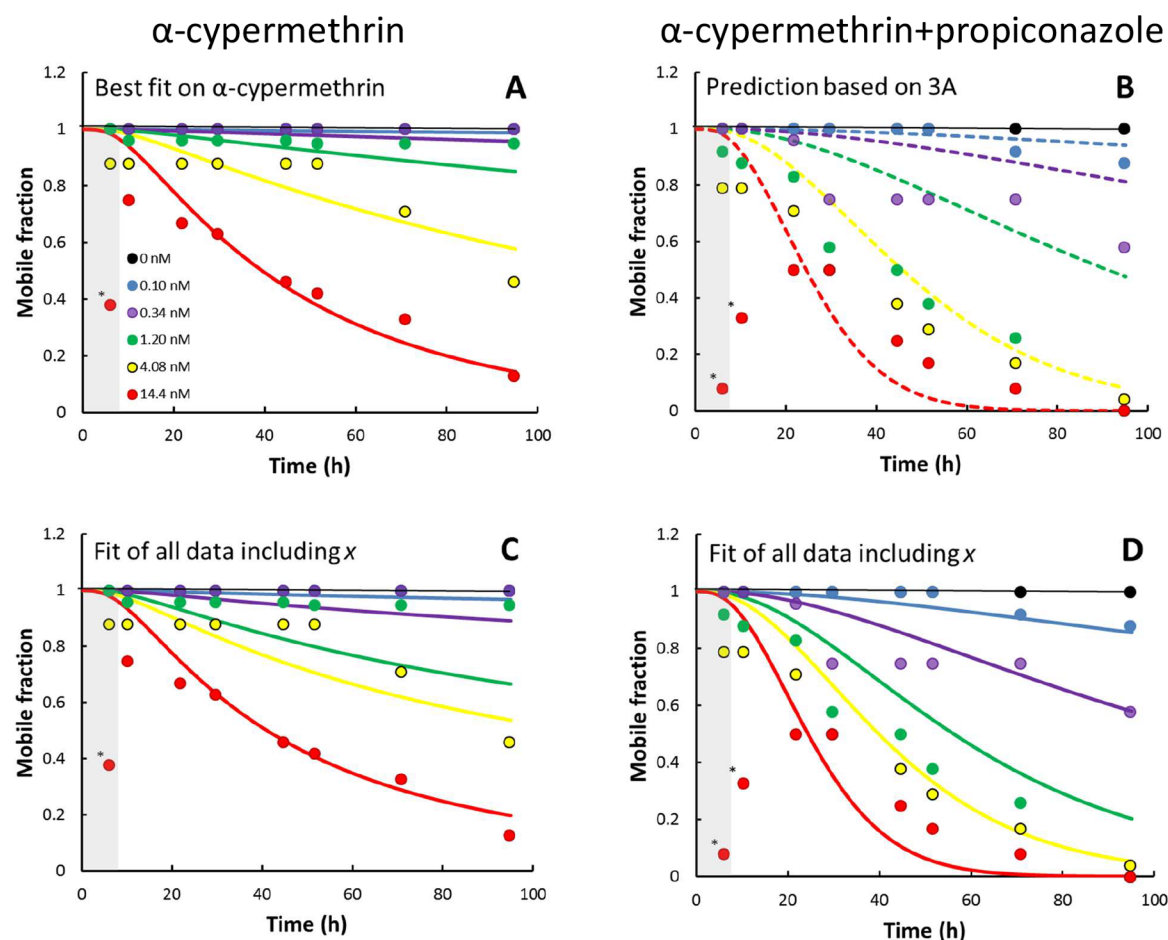


**Figure 3.** Fraction of mobile daphnids ( $n = 24$ ) as a function of time for daphnids being exposed to increasing pulse concentrations (see legend) of  $\alpha$ -cypermethrin with and without coexposure to propiconazole. The pulse exposure duration is marked with gray. Treatments and time points where daphnids were immobilized during the pulse, but recovered mobility, are marked with an asterisk and are not included in the model fits. In (A) and (C), daphnids were exposed to  $\alpha$ -cypermethrin only, while in (B) and (D) daphnids were exposed to the same  $\alpha$ -cypermethrin concentrations but in the presence of  $1.4 \mu\text{M}$  propiconazole. Hence, the treatment with zero  $\alpha$ -cypermethrin in (B) and (D) tests the effect of propiconazole only. Data in (A) are described with the TKTD model (eqs 1–9), and the fit results are shown with solid lines. The dashed lines in Figure B depict model predictions based on the parameters derived from the fit to the pure  $\alpha$ -cypermethrin exposure shown in (A), but including a factor,  $s$ , of 0.113 by which  $\alpha$ -cypermethrin biotransformation is decreased in the presence of propiconazole (eq 4, Table 1). In (A) and (B), we assume uptake rates to be independent of the external concentration and equal to the uptake rates calculated based on the experiment presented in Figure 2, conducted at  $0.54 \text{ nM}$   $\alpha$ -cypermethrin. As the two highest concentrations of  $4.08$  and  $14.4 \text{ nM}$ , however, immobilize the daphnids, it is likely that uptake rates after immobilization are lower than when the daphnids are mobile. In (C) and (D), all data are fitted together to the TKTD model described in eqs 2–9 but substituting eq 1 with eqs 10 and 11. This substitution allows the uptake rates to decrease by a factor  $x$ , when daphnids become immobilized. Immobilisation is set to happen when the internal  $\alpha$ -cypermethrin concentrations reach a certain threshold. Details of the calculation of the internal threshold and the factor  $x$  is given in Figure S4.

data significantly better than the GUTS-IT model, it was decided to use GUTS-SD as the default TD model (see SI B for model comparisons).

The TD-parameters were first determined based on the survival data for daphnids exposed to  $\alpha$ -cypermethrin pulses alone (Table S9). The background hazard,  $h_{b,1}$ , was zero and the threshold for effect,  $z$ , was low and not significantly different from zero and was hence set to zero. The model described the data well and is shown in Figure 3A. In a subsequent step, the survival data of  $\alpha$ -cypermethrin in the presence of propiconazole were predicted based on the model parameters for  $\alpha$ -cypermethrin alone, assuming that the only parameter affected was  $k_{m\_pyr}$ , which was decreased by the factor  $s$ , determined to be 0.113 in the TK-experiment (Figure 1B and Table 1). The model generally under predicted the effect of the three low concentrations while slightly over predicting the effect of the

highest concentration (Figure 3B). As TD parameters of the pure  $\alpha$ -cypermethrin treatment were not determined very accurately, since most treatments did not have an effect on mobility,  $k_{k\_pyr}$  and  $k_{dr\_pyr}$  were fitted based on all data of Figure 3 (panels A and B), keeping  $s$  equal to 0.113. This gave slightly different parameter values (Table S9) but maintained the pattern of overpredicting the effect of high pulse concentrations while under-predicting the effect of low concentrations (Figure S2).

**Testing TK-Model Assumptions.** There could be various reasons for the systematic under predictions at low  $\alpha$ -cypermethrin concentrations, as the present model builds on very crude assumptions far from considering the complexity of living organisms. In the following, we evaluate our assumptions in terms of the TKTD-model.



For the TK, the two main assumptions were (1) that the age of the daphnids does not affect TK parameters and (2) that the TK parameters measured at 0.72 nM  $\alpha$ -cypermethrin (approximately equal to the second lowest concentration in the TD experiment) are independent of the  $\alpha$ -cypermethrin concentration. As the TK data of Figure 1A were measured in 4–7 days old daphnids,<sup>33</sup> and the TD data were based on 4–8 days old daphnids,<sup>1</sup> sizes, and potential dilution by growth should be similar in the two studies. Dilution by growth is therefore implicitly included in the TK parameters. It is, however, likely that growth dilution would depend on the  $\alpha$ -cypermethrin pulse concentration, as we observed that severely intoxicated daphnids grew slower than control daphnids. Unfortunately, growth was not quantitatively measured in the experiments. If a lower growth dilution in severely intoxicated daphnids had been of quantitative importance, a higher mortality than predicted at high  $\alpha$ -cypermethrin would be expected. Since the contrary was the case, differences in growth dilution between treatments were most likely of limited importance.

A more severe age-related assumption is that the activity of the metabolic enzymes given per biomass is constant during the first nonreproducing life-stages of *D. magna*. To confirm the validity of this assumption, we measured P450 activity in *D. magna* as a function of age (Figure S3). The measurements showed a strong linear correlation between activity and size measured both as weight (Figure S3,  $R^2 = 0.97$ ) and protein content (not shown,  $R^2 = 0.97$ ) up to the time of visual egg production (day 6). Hence, the assumption of constant P450 activity per wet weight is valid.

The assumption that TK is concentration-independent could be critical. During the pulse exposure to  $\alpha$ -cypermethrin, daphnids become immobilized at high concentrations (Figure 3). Depicting immobility as a function of the modeled internal  $\alpha$ -cypermethrin concentration at the end of the pulse for the two experiments (Figure S4) show a linear relationship between modeled internal concentrations and daphnid immobility above an internal threshold of  $\sim 213$  pmol g<sup>-1</sup> daphnid FW. If  $\alpha$ -cypermethrin is taken up at a slower rate when daphnids are immobilized then the true internal concentrations in immobilized daphnids will be lower than predicted under the assumption of concentration independent uptake. Belden and Lydy showed increased uptake rates of chlorpyrifos with increasing ventilation rates.<sup>10</sup> In fish, the uptake of hydrophobic chemicals has been shown to be limited by the water flow over the gills.<sup>38</sup> It is therefore very likely that immobility, and the resulting proposed decreased respiration rates, will affect uptake rates. This hypothesis (Figure 1, gray dotted arrow) can be tested by letting the uptake rate  $k_{in\_pyr}$  decrease by a factor,  $x$ , as soon as the internal concentrations surpass the threshold of 213 pmol g<sup>-1</sup> daphnid FW. We incorporated the threshold in the model by having two uptake scenarios.

If  $C_{in\_pyr} < 213$  pmol g<sup>-1</sup> daphnid FW

$$\frac{dC_{in\_pyr}(t)}{dt} = k_{in\_pyr} \times C_{w\_pyr}(t) - k_{out\_pyr} \times C_{in\_pyr}(t) - sk_{m\_pyr} \times C_{in\_pyr}(t) \quad (10)$$

else,

$$\frac{dC_{in\_pyr}(t)}{dt} = xk_{in\_pyr} \times C_{w\_pyr}(t) - k_{out\_pyr} \times C_{in\_pyr}(t) - sk_{m\_pyr} \times C_{in\_pyr}(t) \quad (11)$$

The scenarios for uptake rates with different  $x$  values are shown in Figure S4. Fitting data including  $x$ , improved the fit of the mixture significantly (Table S9, Figure 3D, relative likelihood test,  $p < 0.001$ ). The  $x$  value was fitted to  $0.287 \pm 0.023$ , suggesting that the uptake rate of the pyrethroid in immobilized daphnids is decreased to approximately 30% of the rate of mobile daphnids.

The acute immobility during the pulse may be caused by damage rather than the internal concentration of the pyrethroid. Since mobility recovers immediately after the pulse (Figure 3, panels A and B) proportionately with the decrease of internal concentrations, while damage increases after the pulse (Figure S5), we find that internal concentrations are the most correct measure to use to determine an internal threshold for changes in the uptake rate. Our data suggest that  $\alpha$ -cypermethrin induce effects at several levels: acutely, leading to immobilization, which is most likely a direct result of  $\alpha$ -cypermethrin binding to the sodium receptors of the nerves. This effect, however, seems to be reversible, as a large majority of the daphnids immobilized during the pulse recovered their mobility after being transferred to clean medium. In addition, long-term effects are observed, as the fraction of “re-mobilised” daphnids ultimately die. Hence, the long-term effect seems to be related to long-term damage, which is described in our model by the scaled damage function. Long-term damage has been observed also in other organisms exposed to pyrethroid pulses.<sup>37</sup>

**Testing TD-Model Assumptions.** A wrong assumption concerning toxicodynamics could also have influenced the results. Hence, if we return to our initial assumption about TK (that TK is concentration-independent) and look at TD, the main assumption is that the synergistic mechanism can be explained solely by the change in the biotransformation rate of  $\alpha$ -cypermethrin and that  $\alpha$ -cypermethrin alone is causing the observed toxicity.

Azoles have been shown to disturb sublethal processes such as hormone synthesis and neonate development.<sup>39,40</sup> It could be hypothesized that even though azole concentrations were chosen not to induce any mortality by themselves, their sublethal damage could add to the joint damage or damage recovery and subsequently affect daphnids' survival (Figure 1, gray dotted arrow). As the azole concentration is constant at all pyrethroid treatments, a potential damage inflicted by the azoles would add proportionally more to the joint killing rate at low  $\alpha$ -cypermethrin concentrations compared to their relative contribution in the high  $\alpha$ -cypermethrin treatments. In Ashauer et al., the joint effect of two similarly acting chemicals given in pulses were assessed by adding their relative damage, calculating an average threshold at any point in time.<sup>23</sup> This makes sense for assessing the joint effect of chemicals with the same mode of action, which is not the case in the present study. The approach was nonetheless tried; the propiconazole damage predicted using the parameters of Dalhoff et al.<sup>20</sup> was multiplied with a scaling factor ( $\gamma$ ) to compensate for the different potencies of the chemicals and was added to the  $\alpha$ -cypermethrin damage (see SI C for further details). The fit was not improved significantly by adding the azole damage



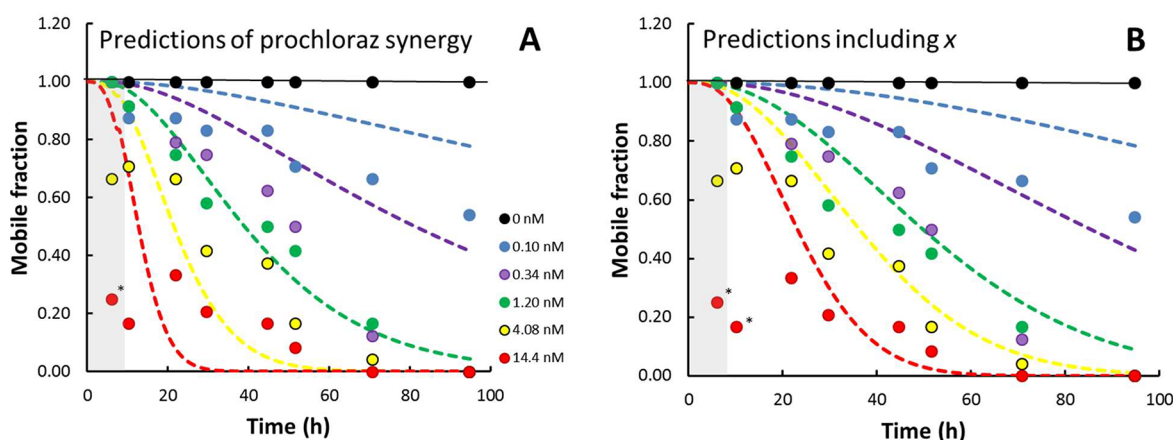


**Figure 4.** Fraction of mobile daphnids ( $n = 24$ ) as a function of time for daphnids being exposed to increasing pulse concentrations of  $\alpha$ -cypermethrin (see legend) in the presence of  $1.3 \mu\text{M}$  prochloraz. The pulse exposure duration is marked with gray. Treatments and time points where daphnids were immobilized during the pulse, but recovered mobility, are marked with an asterisk and are not included in the fits. Data in (A) are predicted with the TKTD model (eq 1–9), using the parameters of daphnids exposed to  $\alpha$ -cypermethrin alone (Figure 3A, Table S9) and a factor,  $s$ , of 0.00025, by which  $\alpha$ -cypermethrin biotransformation is reduced in the presence of prochloraz. In (A), we also assume uptake rates to be independent of the external concentration and equal to the uptake rates calculated based on the experiment presented in Figure 2, conducted at  $0.54 \text{ nM}$   $\alpha$ -cypermethrin. As the two highest concentrations of  $4.08$  and  $14.4 \text{ nM}$ , however, immobilize the daphnids, it is likely that uptake rates after immobilization are lower than when the daphnids are mobile. For the model predictions of (B), eq 1 was substituted with eqs 10 and 11. This substitution allows the uptake rates to decrease by a factor  $x$ , when daphnids become immobilized. Immobilisation is set to happen when the internal  $\alpha$ -cypermethrin concentrations reach a certain threshold. Details of the calculation of the internal threshold and the factor  $x$  is given in Figure S4. All predictions are shown with dashed lines.

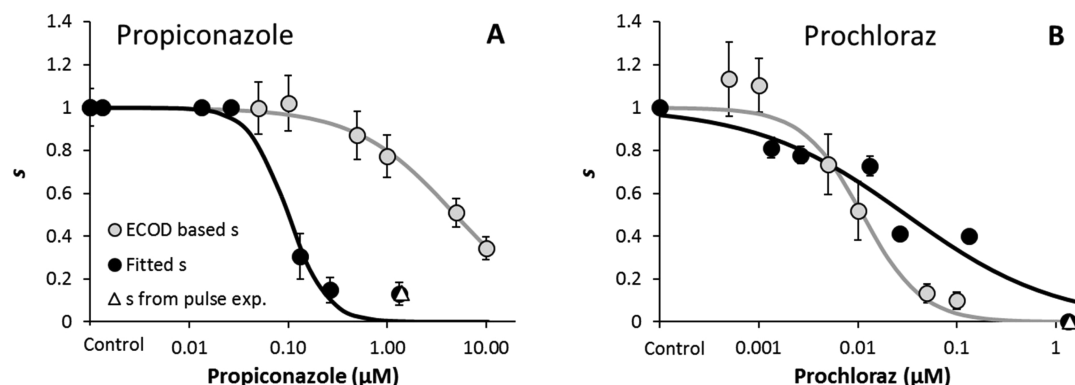


**Figure 5.** Effect of the two azoles: (A) propiconazole and (B) prochloraz on biotransformation rates given by the  $s$  parameter estimated either by measurements of in vivo cytochrome P450 activity inhibition (relative ECOD activity) (gray  $\bullet$  and line) or by fitting the  $s$  parameter to the data of Bjergager et al.<sup>34</sup> (Black  $\bullet$  and line). The  $s$  parameters determined from the pulse experiment of Kretschmann et al.<sup>1</sup> are given as white  $\blacktriangle$ . Data are given  $\pm$  stdev and are described by a log–logistic two parameter model (eq 5). Fit parameters are given in Table S10.

indicated by the higher AIC values (Table S9 and Figures S6 and S7).

**Validating the Model on Prochloraz.** To test the hypothesis that the synergistic potential of other azoles can be described by a TKTD model with the azole affecting  $k_m$  only, we tested both the original model, assuming concentration independent uptake, and the model assuming a decrease in uptake of  $\alpha$ -cypermethrin at high internal concentrations, with the azole prochloraz. Running both models parametrized for propiconazole and only fitting  $s$ , showed that  $s$  approached zero, indicating that prochloraz at a concentration of  $1.3 \mu\text{M}$  completely stopped  $\alpha$ -cypermethrin biotransformation (Figure 4). This is no surprise, as prochloraz is known to be a much stronger synergist and inhibitor of P450 activity compared to propiconazole.<sup>2,20</sup> Measuring in vivo P450 inhibition in *D. magna*, Dalhoff et al. found a 445-fold lower  $\text{IC}_{50}$  for prochloraz compared to propiconazole. Converting this difference in potency to the model inhibition factor  $s$  would decrease its

value from the  $0.113$  estimated for propiconazole to  $0.00025$  for prochloraz, which results in a biotransformation rate very close to zero. Hence, for these two azoles it seems as if the in vivo measurements of their P450 inhibition potential reflect their synergistic potential via the parameter  $s$ , when tested at high constant concentrations.

Of the two models used to describe the data set with prochloraz coexposure, the model assuming decreased uptake rates at high internal  $\alpha$ -cypermethrin concentrations (Figure 4B) described data considerably better compared to the model assuming concentration independent uptake (Figure 4A), giving log-likelihood and AIC values of  $-343$  and  $688$ , and  $-326$  and  $655$  for fits without and with  $x$ , respectively. This strengthens the hypothesis that uptake rates are affected by the paralyzing effect of  $\alpha$ -cypermethrin. Hence, future studies should focus on the effect chemical toxicity can have on chemical uptake and potentially also excretion rates.

### Parameterising $s$ for Variable Azole Concentrations.

Up until now, the model was parametrized on data with constant azole concentration, high enough to ensure synergistic effects. Azole concentrations in the environment do, however, vary.<sup>34</sup> To confirm the hypothesis of azole interference with biotransformation under variable azole exposure, the model was parametrized to a data set with different propiconazole or prochloraz concentrations and the modeled effect on biotransformation given by the  $s$  parameter was compared with measured in vivo cytochrome P450 activity inhibition. Data were first fitted with individual  $s$ -parameters for each azole treatment and with common TD parameters (Table S9). The individually obtained  $s$ -parameters were then described by a two parameter log-logistic model (eq 5, Figure 5), and the obtained parameters were used as starting values for the TD model describing  $s$  as a function of the external azole concentration (SI D, Tables S9 and S10). The survival curves for the combined exposures of three  $\alpha$ -cypermethrin concentrations and seven azole concentrations from the study of Bjergager et al.,<sup>34</sup> where mobility deviates from the controls, are shown in Figures S8 and S9 for propiconazole and prochloraz, respectively. For propiconazole, the TD model describing  $s$  as a function of the external azole concentration did not describe data significantly better than the model with  $s$  being determined individually for each of the three azole concentration inducing synergy (relative likelihood test,  $p = 0.15$ ), whereas it did for prochloraz, where six concentrations induced synergy (relative likelihood test,  $p < 0.001$ ). It is remarkable that the  $s$  parameter determined from the pulse experiments of Kretschmann et al.<sup>1</sup> was almost identical to the  $s$  parameter measured at constant  $\alpha$ -cypermethrin concentrations in the experiments of Bjergager et al.<sup>34</sup> with approximately the same starting concentration (Figure 5). Obtaining an incomplete inhibition of the biotransformation rate at the highest propiconazole concentration in two independent experiments could suggest that full inhibition by propiconazole is not possible.

Comparing the  $s$ -parameter determined by the fits and by measuring in vivo inhibition of ECOD activity showed remarkably good correspondence for prochloraz, confirming that the synergistic potential of prochloraz can be explained by its inhibitory effect on cytochrome P450 ECOD activity. For propiconazole, however, the observed synergistic potential expressed by the fitted  $s$  was much larger than what would be predicted by the ECOD assay (Figure SA). The discrepancy between inhibition potential and synergistic potential for the two azoles was also discussed in Dalhoff et al.,<sup>20</sup> but in that publication synergistic potential was only based on a single azole concentration. The present results suggest that the synergistic potential of propiconazole cannot be solely explained by inhibition of in vivo ECOD activity. Hence, in addition to inhibiting P450 enzymes involved in 7-ethoxycoumarin oxidation, propiconazole could also be proposed to inhibit other enzymes responsible for detoxification of  $\alpha$ -cypermethrin. Alternatively, studies have shown azoles to be broken down to both potentially active and inactive biotransformation products in aquatic invertebrates.<sup>41</sup> The longer duration of the synergy study compared to the inhibition measurements could have resulted in a buildup of active biotransformation products of propiconazole, responsible for the higher potency seen over the 14 day long synergy study compared to the ECOD inhibition potential measured after 18 h of exposure.

**Model Strengths and Weaknesses.** One main finding of the present study is the demonstration that TKTD models are excellent tools to test hypotheses and assumptions concerning chemical interactions in a species as *D. magna*. By modeling the TK-data, we discovered that the measured  $\alpha$ -cypermethrin concentrations in and on the daphnids are better described including a proposed sorption component than with a conventional one-compartment model. This hypothesis can now be experimentally tested. The modeling also showed that the proposed effect of azoles on uptake of  $\alpha$ -cypermethrin did not seem to be of importance for daphnids. The effect of  $\alpha$ -cypermethrin on organisms' mobility during the pulse, however, seems to decrease uptake rates. Hence, toxicant induced changes in behavior should be considered when measuring and modeling toxicokinetics and should be confirmed experimentally. The modeling also revealed that the "damage" killing the daphnids is not the same as the damage affecting behavior, as the latter was best described by the internal concentrations and not by the damage function. Finally, the results confirmed the hypothesis that azole synergy is primarily caused by the effect of the azoles on the biotransformation rate constant of  $\alpha$ -cypermethrin. On the basis of this study, we therefore conclude that TKTD models of interacting mixtures seem to be a promising tool to test mechanisms of interactions between chemicals, creating hypotheses that can be tested experimentally. Their predictive ability on variable exposure scenarios is, however, still to be explored, as is their applicability to other chemical mixtures, as well as other species.

## ■ ASSOCIATED CONTENT

### Supporting Information

The Supporting Information is available free of charge on the ACS Publications website at DOI: 10.1021/acs.est.7b02723.

Summary of material and methods for previously published experiments used for model calibration and validation (SI A), GUTS-IT implementation (SI B), how to add azole damage to the model (SI C) and details of fitting the  $s$  parameter (SI D), tables of exposure concentrations and survival data for all modeled experiments (Table S1–S8), parameter values and AIC for models fit under different assumptions (Table S9 and S10), and figures showing model predictions, modeled data, and data supporting assumptions (Figure S1–S9) (PDF)

## ■ AUTHOR INFORMATION

### Corresponding Author

\*Phone: +45 29611743; email: [ncf@plen.ku.dk](mailto:ncf@plen.ku.dk).

### ORCID

Nina Cedergreen: 0000-0003-4724-9447

Kristoffer Dalhoff: 0000-0001-8615-231X

Michele Gottardi: 0000-0003-0619-8890

### Present Address

<sup>§</sup>Key Laboratory of Pollution Ecology and Environmental Engineering, Institute of Applied Ecology, Chinese Academy of Sciences, 110016 China.

### Notes

The authors declare no competing financial interest.

## ACKNOWLEDGMENTS

This work was supported by a research grant from The Danish Council for Independent Research/Technology and Production Science. Thank you to Roman Ashauer and Tjalling Jager for inspiration and discussions of TKTD models for mixture toxicity assessments and to five anonymous reviewers whose thorough review have improved the manuscript immensely.

## REFERENCES

- (1) Kretschmann, A.; Gottardi, M.; Dalhoff, K.; Cedergreen, N. The synergistic potential of the azole fungicides prochloraz and propiconazole toward a short alpha-cypermethrin pulse increases over time in *Daphnia magna*. *Aquat. Toxicol.* **2015**, *162*, 94–101.
- (2) Norgaard, K. B.; Cedergreen, N. Pesticide cocktails can interact synergistically on aquatic crustaceans. *Environ. Sci. Pollut. Res.* **2010**, *17* (4), 957–967.
- (3) Pilling, E. D.; Bromley-Challanor, K. A. C.; Walker, C. H.; Jepson, P. C. Mechanism of synergism between the pyrethroid insecticide lambda-cyhalothrin and the imidazole fungicide prochloraz in the honeybee (*Apis mellifera* L.). *Pestic. Biochem. Physiol.* **1995**, *51*, 1–11.
- (4) Pilling, E. D.; Jepson, P. C. Synergism between EBI fungicides and a pyrethroid insecticide in the honeybee (*Apis mellifera*). *Pestic. Sci.* **1993**, *39* (4), 293–297.
- (5) Cedergreen, N. Quantifying Synergy: A Systematic Review of Mixture Toxicity Studies within Environmental Toxicology. *PLoS One* **2014**, *9* (5), 1–12.
- (6) Posthuma, L.; Baerselman, R.; Van Veen, R. P. M.; Dirven-Van Breemen, E. M. Single and joint toxic effects of copper and zinc on reproduction of *Enchytraeus crypticus* in relation to sorption of metals in soils. *Ecotoxicol. Environ. Saf.* **1997**, *38* (2), 108–121.
- (7) Elliott, N. G.; Swain, R.; Ritz, D. A. Metal interaction during accumulation by the mussel *Mytilus Edulis Planulatus*. *Mar. Biol.* **1986**, *93* (3), 395–399.
- (8) Mochida, K.; Ito, K.; Harino, H.; Kakuno, A.; Fujii, K. Acute toxicity of pyriithione antifouling biocides and joint toxicity with copper to red sea bream (*Pagrus major*) and toy shrimp (*Heptacarpus futilirostris*). *Environ. Toxicol. Chem.* **2006**, *25* (11), 3058–3064.
- (9) Woznica, Z.; Nalewaja, J. D.; Messersmith, C. G. Sulfosulfuron efficacy is affected by surfactants, pH of spray mixture, and salts. *Pesticide Formulations and Application Systems: A New Century for Agricultural Formulations, Twenty First Volume* **2001**, *1414*, 11–22.
- (10) Belden, J. B.; Lydy, M. J. Impact of atrazine on organophosphate insecticide toxicity. *Environ. Toxicol. Chem.* **2000**, *19* (9), 2266–2274.
- (11) Cedergreen, N.; Kudsk, P.; Mathiasen, S. K.; Streibig, J. C. Combination effects of herbicides on plants and algae: do species and test systems matter? *Pest Manage. Sci.* **2007**, *63* (3), 282–295.
- (12) Walker, C. H. Factors Determining the Toxicity of Organic Pollutants to Animals and Plants. In *Organic Pollutants*, 2nd ed.; CRC Press: London, 2009; pp 17–66.
- (13) Demkovich, M.; Dana, C. E.; Siegel, J. P.; Berenbaum, M. R. Effect of piperonyl butoxide on the toxicity of four classes of insecticides to navel orangeworm (*Amyelois transitella*) (Lepidoptera: Pyralidae). *J. Econ. Entomol.* **2015**, *108* (6), 2753–2760.
- (14) Rodney, S. I.; Teed, R. S.; Moore, D. R. J. Estimating the toxicity of pesticide mixtures to aquatic organisms: A review. *Hum. Ecol. Risk Assess.* **2013**, *19* (6), 1557–1575.
- (15) Johnson, R. M.; Dahlgren, L.; Siegfried, B. D.; Ellis, M. D. Acaricide, fungicide and drug interactions in honey Bees (*Apis mellifera*). *PLoS One* **2013**, *8* (1), 1–10.
- (16) Chalvet-Monfray, K.; Belzunces, L. P.; Colin, M. E.; Fléché, C.; Sabatier, P. Synergy between deltamethrin and prochloraz in bees: modeling approach. *Environ. Toxicol. Chem.* **1996**, *15* (4), 525–534.
- (17) Chalvet-Monfray, K.; Belzunces, L. P.; Colin, M. E.; Fléché, C.; Sabatier, P. Modelling synergistic effects of two toxic agents in the honeybee. *J. Biol. Syst.* **1995**, *03*, 253–263.
- (18) Gottardi, M.; Kretschmann, A.; Cedergreen, N. Measuring cytochrome P450 activity in aquatic invertebrates: a critical evaluation of *in vitro* and *in vivo* methods. *Ecotoxicology* **2016**, *25* (2), 419–430.
- (19) Li, M. H. Development of *in vivo* biotransformation enzyme assays for ecotoxicity screening: *In vivo* measurement of phases I and II enzyme activities in freshwater planarians. *Ecotoxicol. Environ. Saf.* **2016**, *130*, 19–28.
- (20) Dalhoff, K.; Gottardi, M.; Kretschmann, A.; Cedergreen, N. What causes the difference in synergistic potentials of propiconazole and prochloraz toward pyrethroids in *Daphnia magna*? *Aquat. Toxicol.* **2016**, *172*, 95–102.
- (21) Jager, T.; Albert, C.; Preuss, T. G.; Ashauer, R. General unified threshold model of survival - a toxicokinetic-toxicodynamic framework for ecotoxicology. *Environ. Sci. Technol.* **2011**, *45* (7), 2529–2540.
- (22) Ashauer, R.; Thorbek, P.; Warinton, J. S.; Wheeler, J. R.; Maund, S. A method to predict and understand fish survival under dynamic chemical stress using standard ecotoxicity data. *Environ. Toxicol. Chem.* **2013**, *32* (4), 954–965.
- (23) Ashauer, R.; Boxall, A. B. A.; Brown, C. D. Modeling combined effects of pulsed exposure to carbaryl and chlorpyrifos on *Gammarus pulex*. *Environ. Sci. Technol.* **2007**, *41* (15), 5535–5541.
- (24) Godin, S. J.; Crow, J. A.; Scollon, E. J.; Hughes, M. F.; Devito, M. J.; Ross, M. K. Identification of rat and human cytochrome P450 isoforms and a rat serum esterase that metabolize the pyrethroid insecticides deltamethrin and esfenvalerate. *Drug Metab. Dispos.* **2007**, *35* (9), 1664–1671.
- (25) Anand, S. S.; Bruckner, J. V.; Haines, W. T.; Muralidhara, S.; Fisher, J. W.; Padilla, S. Characterization of deltamethrin metabolism by rat plasma and liver microsomes. *Toxicol. Appl. Pharmacol.* **2006**, *212* (2), 156–166.
- (26) Ross, M. K.; Borazjani, A.; Edwards, C. C.; Potter, P. M. Hydrolytic metabolism of pyrethroids by human and other mammalian carboxylesterases. *Biochem. Pharmacol.* **2006**, *71* (5), 657–669.
- (27) Correia, M. A.; Ortiz, P. R. Inhibition of Cytochrome P450 Enzymes. In *Cytochrome P450*, 3rd ed.; Ortiz de Montellano, P. R., Ed.; Springer: New York, 2005; pp 247–322.
- (28) Copping, L. G.; Hewitt, H. G. *Chemistry and Mode of Action of Crop Protection Agents*, 1st ed.; The Royal Society of Chemistry: Cambridge, U.K., 1998; Vol. 1; pp 1–145.
- (29) Ashauer, R.; Agatz, A.; Albert, C.; Ducrot, V.; Galic, N.; Hendriks, J.; Jager, T.; Kretschmann, A.; O'Connor, I.; Rubach, M. N.; Nyman, A. M.; Schmitt, W.; Stadnicka, J.; van den Brink, P. J.; Preuss, T. G. Toxicokinetic-Toxicodynamic modeling of quantal and graded sublethal endpoints: A brief discussion of concepts. *Environ. Toxicol. Chem.* **2011**, *30* (11), 2519–2524.
- (30) Ashauer, R.; O'Connor, I.; Hintermeister, A.; Escher, B. I. Death dilemma and organism recovery in ecotoxicology. *Environ. Sci. Technol.* **2015**, *49* (16), 10136–10146.
- (31) Ashauer, R.; Albert, C.; Augustine, S.; Cedergreen, N.; Charles, S.; Ducrot, V.; Focks, A.; Gabsi, F.; Gergs, A.; Goussen, B.; Jager, T.; Kramer, N. I.; Nyman, A. M.; Poulsen, V.; Reichenberger, S.; Schafer, R. B.; van den Brink, P. J.; Veltman, K.; Vogel, S.; Zimmer, E. I.; Preuss, T. G. Modelling survival: exposure pattern, species sensitivity and uncertainty. *Sci. Rep.* **2016**, *6*, 1–11.
- (32) Rubach, M. N.; Ashauer, R.; Maund, S. J.; Baird, D. J.; van den Brink, P. J. Toxicokinetic variation in 15 freshwater arthropod species exposed to the insecticide chlorpyrifos. *Environ. Toxicol. Chem.* **2010**, *29* (10), 2225–2234.
- (33) Kretschmann, A.; Cedergreen, N.; Christensen, J. H. Measuring internal azole and pyrethroid pesticide concentrations in *Daphnia magna* using QuEChERS and GC-ECD-method development with a focus on matrix effects. *Anal. Bioanal. Chem.* **2016**, *408* (4), 1055–1066.
- (34) Bjergager, M. B. A.; Dalhoff, K.; Kretschmann, A.; Norgaard, K. B.; Mayer, P.; Cedergreen, N. Determining lower threshold concentrations for synergistic effects. *Aquat. Toxicol.* **2017**, *182*, 79–90.
- (35) Burnham, K. P.; Anderson, D. R. *Model Selection and Multimodel Inference: A Practical Information-Theoretic Approach*, 2nd ed.; Springer-Verlag, 2002.
- (36) Bjergager, M. A. Azole Fungicides As Synergists in the Aquatic Environment. Ph.D. Thesis, University of Copenhagen, 2015.

(37) Rasmussen, J. J.; Wiberg-Larsen, P.; Kristensen, E. A.; Cedergreen, N.; Friberg, N. Pyrethroid effects on freshwater invertebrates: A meta-analysis of pulse exposures. *Environ. Pollut.* **2013**, *182*, 479–485.

(38) Nichols, J. W.; Mckim, J. M.; Andersen, M. E.; Gargas, M. L.; Clewell, H. J.; Erickson, R. J. A physiologically based toxicokinetic model for the uptake and disposition of waterborne organic-chemicals in fish. *Toxicol. Appl. Pharmacol.* **1990**, *106* (3), 433–447.

(39) Hassold, E.; Backhaus, T. The predictability of mixture toxicity of demethylase inhibiting fungicides to *Daphnia magna* depends on life-cycle parameters. *Aquat. Toxicol.* **2014**, *152*, 205–214.

(40) Hassold, E.; Backhaus, T. Chronic toxicity of five structurally diverse demethylase-inhibiting fungicides to the crustacean *Daphnia magna*: A comparative assessment. *Environ. Toxicol. Chem.* **2009**, *28* (6), 1218–1226.

(41) Rosch, A.; Anliker, S.; Hollender, J. How biotransformation influences toxicokinetics of azole fungicides in the aquatic invertebrate *Gammarus pulex*. *Environ. Sci. Technol.* **2016**, *50* (13), 7175–7188.